AIP | Journal of Applied Physics

Relaxation and critical strain for maximum In incorporation in AlInGaN on GaN grown by metal organic vapour phase epitaxy

Benjamin Reuters, M. Finken, A. Wille, B. Holländer, M. Heuken et al.

Citation: J. Appl. Phys. **112**, 093524 (2012); doi: 10.1063/1.4764342
View online: http://dx.doi.org/10.1063/1.4764342
View Table of Contents: http://jap.aip.org/resource/1/JAPIAU/v112/i9
Published by the American Institute of Physics.

Additional information on J. Appl. Phys.

Journal Homepage: http://jap.aip.org/
Journal Information: http://jap.aip.org/about/about_the_journal
Top downloads: http://jap.aip.org/features/most_downloaded
Information for Authors: http://jap.aip.org/authors

ADVERTISEMENT

Downloaded 16 May 2013 to 134.94.122.141. This article is copyrighted as indicated in the abstract. Reuse of AIP content is subject to the terms at: http://jap.aip.org/about/rights_and_permissions

Relaxation and critical strain for maximum In incorporation in AlInGaN on GaN grown by metal organic vapour phase epitaxy

Benjamin Reuters,[1,2,a)] M. Finken,[1,2] A. Wille,[1,2] B. Holländer,[2,3] M. Heuken,[1,4] H. Kalisch,[1,2] and A. Vescan[1,2]
[1]*RWTH Aachen University, GaN Device Technology, Sommerfeldstrasse 24, 52074 Aachen, Germany*
[2]*Jülich Aachen Research Alliance, JARA-FIT, Wilhelm-Johnen-Straße, 52428 Jülich*
[3]*Forschungszentrum Jülich GmbH, PGI9-IT, 52425 Jülich, Germany*
[4]*AIXTRON SE, Kaiserstr. 98, 52134 Herzogenrath, Germany*

(Received 12 June 2012; accepted 12 October 2012; published online 13 November 2012)

Quaternary AlInGaN layers were grown on conventional GaN buffer layers on sapphire by metal organic vapour phase epitaxy at different surface temperatures and different reactor pressures with constant precursor flow conditions. A wide range in compositions within 30–62% Al, 5–29% In, and 23–53% Ga was covered, which leads to different strain states from high tensile to high compressive. From high-resolution x-ray diffraction and Rutherford backscattering spectrometry, we determined the compositions, strain states, and crystal quality of the AlInGaN layers. Atomic force microscopy measurements were performed to characterize the surface morphology. A critical strain value for maximum In incorporation near the AlInGaN/GaN interface is presented. For compressively strained layers, In incorporation is limited at the interface as residual strain cannot exceed an empirical critical value of about 1.1%. Relaxation occurs at about 15 nm thickness accompanied by strong In pulling. Tensile strained layers can be grown pseudomorphically up to 70 nm at a strain state of 0.96%. A model for relaxation in compressively strained AlInGaN with virtual discrete sub-layers, which illustrates the gradually changing lattice constant during stress reduction is presented. © *2012 American Institute of Physics*. [http://dx.doi.org/10.1063/1.4764342]

I. INTRODUCTION

Epitaxial growth of ternary AlGaN, AlInN, InGaN, and quaternary AlInGaN on GaN has become a very important process because of their use in several types of device structures. The internal polarization fields and resulting interface charges in AlGaN/GaN and AlInN/GaN heterostructures enable the realization of GaN-based high electron mobility transistors (HEMT).[1–3] InGaN is already established in conventional light emitting diodes (LED) and commercialized in several multi-media applications.[4] Alternatively, quaternary AlInGaN has reached the focus of interest because of its versatility in adjusting material properties, i.e., bandgap and lattice constant, separately.[5,6] This offers unique opportunities for polarization-engineered nitride heterostructures, like enhancement-mode HEMT or LED structures without emission wavelength shift.[7–11]

In this work, we investigate the influence of deposition conditions on the composition and structural properties of AlInGaN. Especially, to understand polarization effects in nitride heterostructures, a deeper comprehension of strain and relaxation in these layers is necessary.

II. EXPERIMENTAL DETAILS

The heterostructures investigated in this work were deposited on 2-in. c-plane sapphire substrates in an AIXTRON metal organic vapour phase epitaxy (MOVPE) reactor with standard precursors trimethylaluminum (TMAl), trimethylindium (TMIn), trimethylgallium (TMGa), and ammonia. For AlInGaN layers, nitrogen (N_2) was used as carrier gas, whereas for all In-free layers hydrogen (H_2) was used. Full spectroscopic *in-situ* measurement of the reflectance at different wavelengths between 276 nm and 775 nm by a measurement tool from LayTec with addional true-temperature pyrometer module let us control the growth surface temperature and the growth rate during epitaxy.

A set of relatively thick (30–75 nm) AlInGaN layers were grown on a buffer structure, which consists of a 3.0 μm GaN buffer layer (1060 °C, 300 hPa) on 300 nm high-temperature (1250 °C, 25 hPa) AlN and 7 nm low-temperature (760 °C, 50 hPa) AlN nucleation layer. For all AlInGaN samples, the TMAl, TMIn, and TMGa flows were kept constant at 20.9 μmol/min, 31.5 μmol/min, and 8.8 μmol/min, respectively. While for GaN growth at 1050 °C, a V/III ratio of 1016 is employed, a rather high V/III ratio of 2188 is employed for AlInGaN growth to account for the weaker cracking efficiency of ammonia at lower growth temperatures.[12] Two epitaxial growth parameters were varied to deposit AlInGaN layers with different compositions, the growth surface temperature, and the reactor pressure. A series of five samples were grown, in which either the growth surface temperature or the reactor pressure was kept constant: first, a series of three samples A, B, and C at a constant temperature of 750 °C and different pressures from 70 hPa to 200 hPa; second, a series of three samples D, A, and F grown at constant pressure of 70 hPa and varying temperature from 722 °C to 813 °C.

Access to the AlInGaN thickness, the exact depth-resolved composition, and a benchmark for crystallinity were established by Rutherford backscattering spectrometry

[a)]Author to whom correspondence should be addressed. Electronic mail: reuters@gan.rwth-aachen.de.

 © 2012 American Institute of Physics

Downloaded 16 May 2013 to 134.94.122.141. This article is copyrighted as indicated in the abstract. Reuse of AIP content is subject to the terms at: http://jap.aip.org/about/rights_and_permissions

(RBS) and RBS channelling using 1.4 MeV He^+ ions at a scattering angle of 170°. Channeling spectra were measured after alignment of the [0001] sample normal with respect to the incoming ion beam. Details of the experimental setup were reported elsewhere.[13] Structural characterization on lattice constants and relaxation was performed by high-resolution x-ray diffraction (HRXRD). Morphological investigations were carried out by atomic force microscopy (AFM).

III. RESULTS AND DISCUSSION

Table I gives an overview of reactor conditions and structural properties of all AlInGaN samples investigated here. The reactor pressure $P_{Reactor}$, growth surface temperature $T_{Surface}$, composition, channeling value $\chi_{RBS,min}$, layer thickness, and growth rate are given for each sample. The reactor pressure mainly affects the composition of AlInGaN samples A, B, and C by changing the ratio of the Al to Ga content, as obvious in Table I and also shown in the upper plot of Figure 1. The Al content is decreasing strongly for pressures above 125 hPa. The higher reactor pressures advance gas phase prereactions of TMAl and NH_3, which lead to less Al incorporation and a reduced growth rate to 58% of the growth rate value achieved at low pressure of 70 hPa.[14–16] The In content remains almost constant in this series, which suggests that pressure has little effect on In incorporation in this temperature range.

The bottom plot of Figure 1 shows the RBS channeling values $\chi_{RBS,min}$ for different reactor pressures. Low RBS channeling values $\chi_{RBS,min}$ reflect high crystal quality, as it is observed for sample A. Higher $\chi_{RBS,min}$ values are observed for samples grown at higher pressures, which illustrates an inferior crystal quality, due to disorder, inhomogeneities, interstitials, or impurities. It might also be important to consider a larger gas phase particle concentration due to TMAl prereactions at higher pressures. Nevertheless, the observed channeling values $\chi_{RBS,min}$ between 3% and 8% indicate quite good crystal quality, achieved at a relatively low temperature of 750 °C. A higher defect density might arise due to the larger nominal and residual in-plane strain $\varepsilon_{xx,nom/res}$, which is generated by the larger lattice mismatch to GaN. The nominal strain $\varepsilon_{xx,nom}$ is calculated with Eq. (1) with nominal lattice constants calculated with Vegard's law, taking the composition from RBS into account, and the assumption of a fully strained layer. The residual strain $\varepsilon_{xx,res}$ is calculated with lattice constants derived by HRXRD (10-15) reciprocal space mappings (RSM)

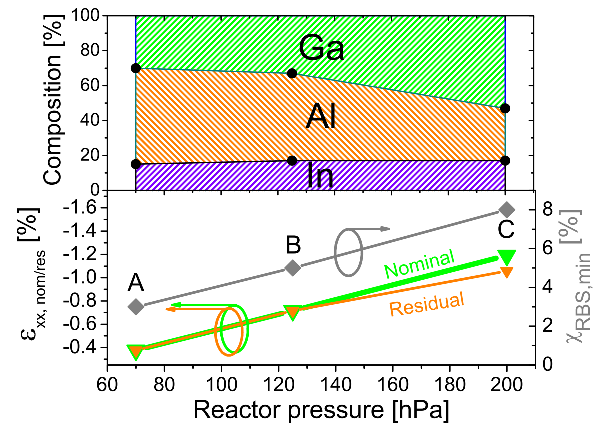

FIG. 1. Compositions determined by RBS (upper plot), nominal strain, residual strain, and $\chi_{RBS,min}$ channeling values (bottom plot) for different reactor pressures.

$$\varepsilon_{xx,nom/res} = \frac{a_{AlInGaN,strained/relaxed} - a_{AlInGaN,nom}}{a_{AlInGaN,nom}}. \quad (1)$$

The nominal and residual strain, also plotted in the bottom plot of Figure 1, shows a similar increasing trend as $\chi_{RBS,min}$ for different reactor pressures, due to the lowered Al contents for higher reactor pressures. The samples A and B are grown pseudomorphically with a nominal and residual strain of −0.38% and −0.72%, respectively. The nominal strain of sample C reaches a quite high value of 1.19%. For this 30 nm thick sample, the XRD (10-15) RSM taken with an open detector and shown in Figure 2 reveals a shift of the AlInGaN peak to lower Q_x values, which indicates partial relaxation of this 30 nm thick layer. This is in agreement with theoretical calculations, which predict a critical thickness of about 8 nm at this strain state for InGaN layers.[17] The theoretical position of a fully strained and fully relaxed layer is also shown. The relaxation in this layer is accompanied by a slight In pulling of about 2% in growth direction, revealed by RBS (not shown here). Taking this into account, the relaxation of this layer, derived by HRXRD analysis and RBS, is in the range of 35% at the surface at 19% In, which leads to a residual strain of a high value of about 1.06%. In order to study the impact of maximum In incorporation on strain generation and relaxation, a further sample series with even higher In contents is presented. Starting from the conditions of sample A grown at 70 hPa, which delivers the best crystal quality of AlInGaN, we investigate the influence of the growth surface temperature on composition and relaxation in AlInGaN. The temperature was changed to a higher

TABLE I. Reactor conditions and structural properties of the investigated samples: Growth surface temperature, reactor pressure, RBS composition, $\chi_{RBS,min}$ values, thickness, and growth rate.

ID	$T_{Surface}$ (°C)	$P_{Reactor}$ (hPa)	Al (%)	In (%)	Ga (%)	$\chi_{RBS,min}$ (%)	Thickness (nm)	r_{Growth} (nm/min)
A	750	70	55	15	30	3	52	5.2
B	750	125	50	17	33	5	34	3.4
C	750	200	30	17	53	8	30	3.0
D	813	70	62	5	33	2	70	4.7
A	750	70	55	15	30	3	52	5.2
E	722	70	48	29	23	22	75	5.0

Downloaded 16 May 2013 to 134.94.122.141. This article is copyrighted as indicated in the abstract. Reuse of AIP content is subject to the terms at: http://jap.aip.org/about/rights_and_permissions

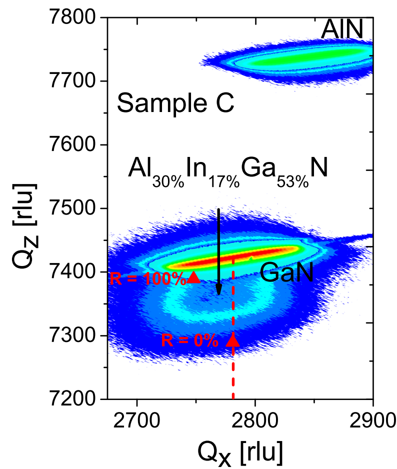

FIG. 2. XRD (10-15) RSM taken with an open detector of sample C. The dashed red line in the image illustrates the Q_x position of the GaN buffer peak. The red triangles illustrate the theoretical position of sample C assumed to be pseudomorphically grown (R = 0%) or fully relaxed (R = 100%).

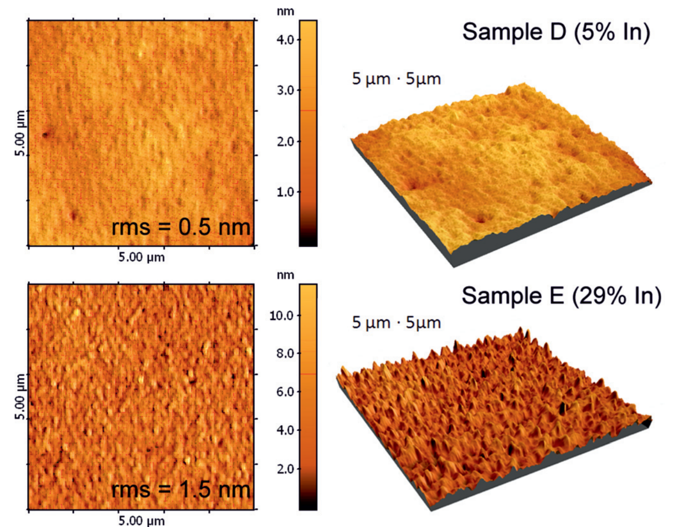

FIG. 3. AFM 5 $\mu m \cdot 5\ \mu m$ scans of sample D (top) and sample E (bottom) in planar illustration (left) and 3D perspective (right) to visualize the difference in morphology.

value of 813 °C (HT) for sample D and to a lower value of 722 °C (LT) for sample E. Worth mentioning here is the very low $\chi_{RBS,min}$ value of sample D, which displays the excellent MOVPE conditions for this layer. Comparison of the two high-quality AlInGaN layers A ($\chi_{RBS,min} = 3\%$) and D ($\chi_{RBS,min} = 2\%$) lets us conclude that a temperature reduction mainly affects In incorporation. Layers with an In content up to 15% exhibit good crystal quality. For sample E grown at an even lower temperature of 722 °C, the In content reaches a high value of up to 29%, due to a lower desorption rate of In atoms because of the weaker bond strength in comparison with those of Al and Ga.[18] In several prior experimental studies, the impact of the growth surface temperature on the composition of AlInGaN was investigated.[19] A linear temperature dependence was found for the In content and can be confirmed with these results. The Al to Ga content ratio only slightly changes with temperature by about 10%. Interesting to note is that the growth rate of sample E is higher than that of sample D. The higher growth rate at low temperatures might be explained by the larger number of In atoms, which are incorporated additionally to Al and Ga in the layer. All results concerning the compositional changes and growth rates are in good aggreement with previous observations.[19] A rather high channeling value $\chi_{RBS,min}$ of 22% for sample E indicates the moderate crystal quality of this layer, which can be explained by the low surface temperature and the resulting high In content. However, in comparison to pure AlInN layers with similar In contents, the quaternary layers appear to have a better crystal quality likely due to the Ga content, which might enhance miscibility and suppress phase separation in AlInGaN.[20,21]

AFM measurements are shown in Figure 3 for sample D with a low In content of 5% and sample E with a high In content of up to 29%. A clear change from a smooth surface with step flow pattern for sample D to the hillock-like morphology of sample E is observed. The transition from 2D growth during epitaxy at high temperatures to 3D growth at low temperatures is likely responsible for the morphology change similar to ternary In-containing layers like InGaN and AlInN.[20,22,23] The enhanced clustering tendency for higher In contents, lower surface diffusion of In atoms and local inhomogeneous compressive strain relaxation might be the most dominant factors for that morphology change. A further indication of the lower crystal quality at lower surface temperatures is the increased root mean square (rms) roughness from 0.5 nm for sample D to 1.5 nm for sample E.

In Figure 4, all samples are plotted in the bandgap vs. lattice constant diagramm. All compositions were determined by RBS (Table I), and the lattice constants were calculated with Vegard's law and the bandgap with a non-weighted bandgap equation

$$E_{g,AlInGaN} = x_{AlN} \cdot E_{g,AlN} + x_{InN} \cdot E_{g,InN} + x_{GaN} \cdot E_{g,GaN} - b_{AlGaN} \cdot x_{AlN} \cdot x_{GaN} - b_{AlInN} \cdot x_{AlN} \cdot x_{InN} - b_{InGaN} \cdot x_{InN} \cdot x_{GaN}. \quad (2)$$

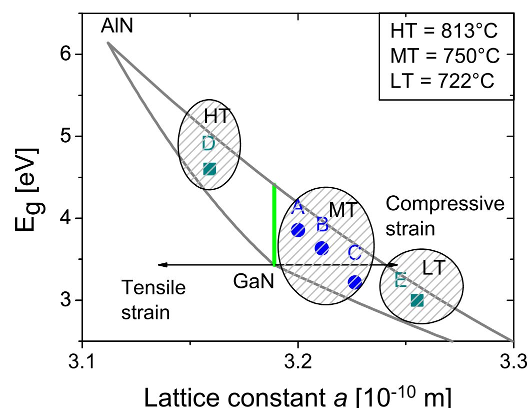

FIG. 4. Calculated AlInGaN bandgaps, employing the compositions determined by RBS, plotted over the lattice constant a, calculated with Vegard's law, for all samples. Samples A, B, and C grown at moderate temperature (MT) and various reactor pressures are plotted in blue circles. Samples grown at either low temperature (LT) or high temperature (HT) and 70 hPa are plotted in cyan squares.

Downloaded 16 May 2013 to 134.94.122.141. This article is copyrighted as indicated in the abstract. Reuse of AIP content is subject to the terms at: http://jap.aip.org/about/rights_and_permissions

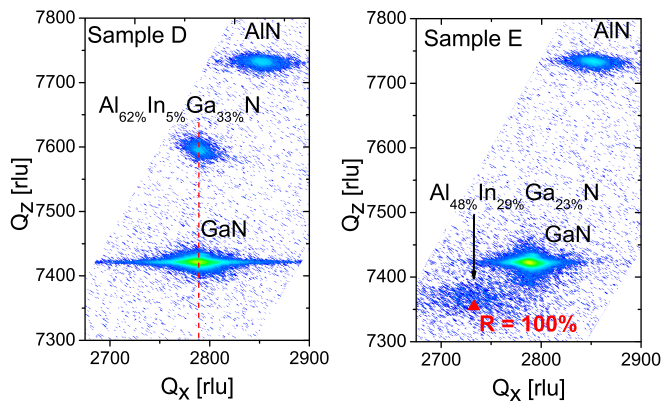

FIG. 5. HRXRD (10-15) RSM of samples D (left) and E (right). The patterned red line in the left image illustrates the equal Q_x position of the AlInGaN peak and GaN buffer peak. The red triangle in the right image is the theoretical position of sample E assumed to be fully relaxed.

Here, E_g is the bandgap of the nitride alloy, x the normalized content of the metal atoms, and b the bowing parameters for ternary alloys. In this paper, we use bowing parameters of 0.9 eV for AlGaN,[24] 1.65 eV for InGaN,[24] and a quite high and constant value of 5.2 eV for AlInN. Especially, the last value fits the bandgaps of pure AlInN barrier layers from our group very well and is consistent with other publications from other groups.[25,26] Bowing parameters for AlInN between 3 eV and above 6 eV are published and still under discussion. The bowing parameter for AlInN might also be dependent on the In content, especially for the In-rich region, in which the bandgap shrinks below the GaN bandgap.[24,27] It is obvious in Figure 4 that all samples, except sample D, are compressively strained. The compressive strain increases either due to the higher In content for lower growth temperatures or due to a lower Al to Ga content ratio for higher reactor pressures. As discussed above, an increasing compressive strain might also contribute to the morphology change from 2D to 3D growth and higher roughnesses.

Figure 5 presents HRXRD (10-15) RSM for samples D and E. For the tensile strained sample D, one can see that the AlInGaN peak of the reciprocal lattice point (RLP) lies vertically on a line with the GaN buffer, which indicates pseudomorphic growth for this 70 nm thick layer. From HRXRD (0004) and (20-24) RSM, the lattice constants were determined to be $a = 3.181$ nm and $c = 5.073$ nm. Further, the ratio of out-of-plane and in-plane strain is determined to be -0.536 for this pseudomorphically grown layer. Elastic constants for wurtzite AlN, GaN, and InN have been obtained by means of density-functional analysis in several studies and are still controversial.[28–30] However, the observed strain ratio is in very good agreement with a theoretical value for $-2C_{13}/C_{33} = -0.540$ with C_{ii} calculated with a recently published composition-dependent formula with bowing parameters.[30] This is a further indication that sample D exhibits high crystal quality with very good miscibility, as the theoretical model takes a homogeneous contribution of Al, In, and Ga atoms into account.

A completely different appearance is found in the RSM for sample E in Figure 5. Here the peak of the quaternary reciprocal lattice point is positioned at a different Q_x value than GaN. This indicates an incoherent growth for most of the layer thickness. The reflection is shifted to lower Q_x and higher Q_z values, which corresponds to a larger lattice constant a and smaller lattice constant c consistent with elastic relaxation. Relaxation of this theoretically highly compressively strained layer likely occurs early during growth, because the highest intensity is observed near the fully relaxed position, which is marked by a red triangle. The relative difference between the nominal in-plane lattice constant, calculated from RBS composition with Vegard's law, and the lattice constant, determined by HRXRD (10-15) reciprocal space mapping is in the range of 10^{-4}, which shows the excellent aggreement of RBS and HRXRD results. Furthermore, it is obvious that the peak of sample E grown at LT is broadened and less intense than that of sample D grown at HT, which indicates the lower crystal quality of this layer determined already by RBS.

The random and the aligned channelling RBS spectra for sample E are shown in Figure 6. In contrast to the HT-grown sample D, which contains very homogeneous In contents over the whole thickness (not shown here), sample E shows an inhomogeneous composition in growth direction. The random RBS measurement exhibits a lower In signal at the AlInGaN/GaN interface in relation to the surface. This is a clear indication for In pulling with increasing thickness of the quaternary layer. The In pulling effect is known for compressively strained InGaN layers.[31] Here, In pulling is assumed to emerge from relaxation in this layer, which increases the in-plane lattice constant. Thus, In atoms can be incorporated more easily. Taking the composition at the surface from RBS of 29% In, 48% Al, and 23% Ga, the lattice mismatch to GaN can be calculated with Eq. (1) to 2.04%. This high strain value might be energetically unfavorable to be established in a thin lateral homogeneous nitride film, which explains why a high average In content cannot be incorporated near the interface.

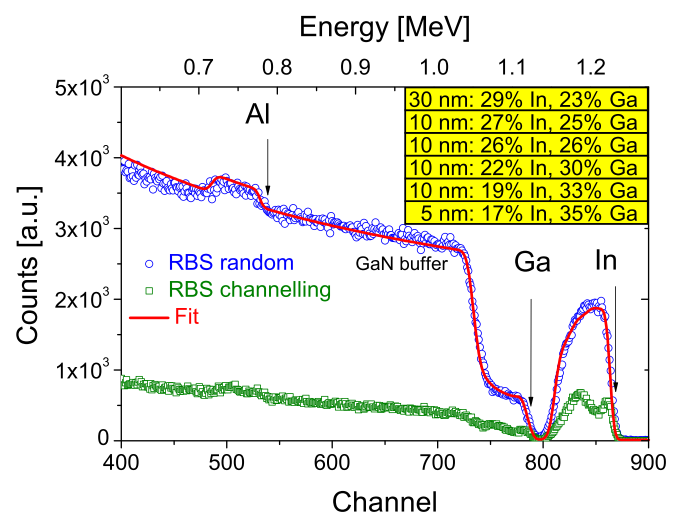

FIG. 6. RBS spectrum of sample E grown at LT. The blue dots represent the random measurement, the green squares represent the channeling signal, and the red curve is a simulation of a multi-layer structure with changing In and Ga contents. The inset illustrates the multi-layered AlInGaN barrier.

Downloaded 16 May 2013 to 134.94.122.141. This article is copyrighted as indicated in the abstract. Reuse of AIP content is subject to the terms at: http://jap.aip.org/about/rights_and_permissions

In order to fit the experimental curve of the RBS measurement shown in Figure 6, a virtual multi-layer structure was assumed for sample E, as a homogeneous AlInGaN composition does not fit the RBS measurement well. A discrete six-fold layer model is most effective in order to be consistent with the measurement curve, while still having a low number of sub-layers to adjust. A higher number of sub-layers would increase accuracy but also the complexity. To further improve the fitting, the increment of the sub-layer thickness is not constant. Near the interface the sub-layer is just 5 nm thick, followed by four 10 nm sublayers and a final 30 nm sub-layer. The simulation of this six-fold layer structure with In contents starting from 19% and increasing to 29% is in very good agreement to the measured curve. The increasing In content is accompanied by a decreasing Ga content from 35% to 23%, which is clearly visible in the intensity decrease of the Ga signal located at channel 750-790 on the right side of the edge of the GaN buffer signal. A constant Al content of 48% is assumed for the whole layer, which is consistent with the measurement. It seems that In atoms, which are adsorbed on the surface, compete with Ga atoms and that the In incorporation is controlled by the highest possible strain. This assumption is plausible because of the tendency of AlGaN layers to prefer Ga-terminated surfaces and In-containing layers to prefer In-terminated surfaces.[32,33] If we take this multi-layer AlInGaN stack as the fitting model for simulating the 2Θ-ω (0002) HRXRD scan, shown in Figure 7, it is possible to gain information about the relaxation processes in this layer. Neither a completely non-relaxed nor a fully relaxed layer fits the HRXRD scan well (not shown here). It is necessary to split the layer into sub-layers and adjust the relaxation for each sub-layer. Although only weak fringe oscillations are observed due to an inferior crystal quality and a diffuse interface, the envelope of the multi-layer fit is perfectly consistent with the HRXRD scan as shown in Figure 7.

To illustrate the strain state of the sub-layers, relaxation and a graded In content derived from our virtual multi-layer model are plotted in the lower part of Figure 8 as a function

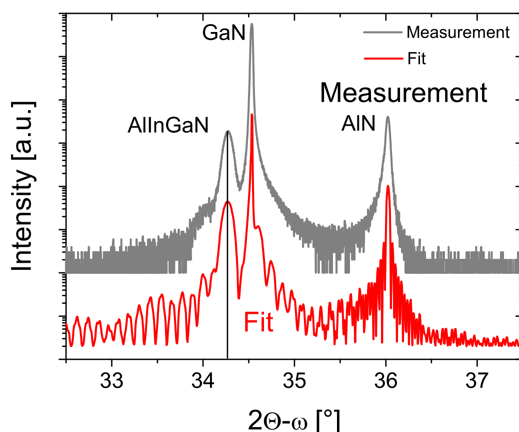

FIG. 7. HRXRD 2Θ-ω scan for sample E grown at LT (grey curve). Also shown is the fitting of the measurement with the six-fold multi-layer model, derived from RBS. Although no interface fringes are observed due to an inferior crystal quality and a diffuse interface, the envelope of the fit is in perfect agreement with the measured scan.

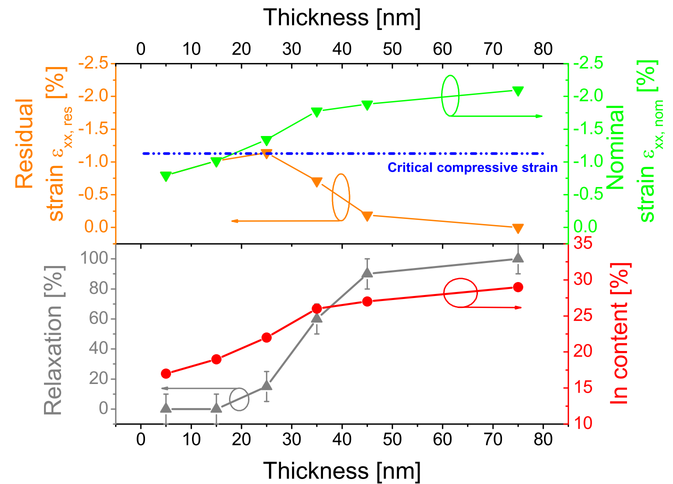

FIG. 8. Relaxation (grey curve), In content (red curve), nominal strain (green curve), and residual strain (orange curve) as functions of the AlInGaN layer thickness for sample E.

of the layer thickness. The values are given at the half thickness for each sub-layer and connected to a continuous function, as this might generate an easily interpreted image to reflect reality most accurately. Relaxation can be adjusted within a variation of 10% in each layer to fit the HRXRD scan. Several aspects are obvious in the bottom plot. The first grown 15 nm with an In content of 17% to 19% can be assumed fully strained. Then, the layer starts to relax and reaches full relaxation at 45 nm with 27% In. It can be clearly seen that the enhanced In incorporation is directly correlated to the relaxation and shows an increase from 17% at the interface to 29% at the surface. The In content at the interface remains low to reduce the lattice mismatch to GaN, which allows a coherent growth on GaN up to a critical thickness.[17] As the critical thickness is exceeded and the lattice starts to relax, the In atoms have the tendency to segregate to these relaxed areas, which leads to a higher In incorporation. These observations are in agreement with results presented for thick InGaN layers, in which In pulling occurs and the In incorporation at the interface is limited by the strain energy.[31,34]

These observations also confirm that the uppermost part of the AlInGaN layer, which is fully relaxed, is dominant in HRXRD mapping analysis. The lower layers might change the lattice constants continuously, so constructive interference for these layers is very weak. This explains the lower intensity of the AlInGaN reciprocal lattice point of sample E in relation to that of sample D. Additionally, the continuously changing AlInGaN composition makes the barrier package undefined and inhibits the appearance of fringe oscillations in the 2Θ-ω (0002) HRXRD scan.

The upper plot in Figure 8 shows the in-plane nominal strain $\varepsilon_{xx,nom}$, which is calculated with Eq. (1) with the assumption of a fully strained layer, and the residual strain $\varepsilon_{xx,res}$, which takes the relaxation determined by HRXRD into account.

The nominal strain increases from -0.80% to above -2% due to strong In pulling. The residual strain near the interface starts with the same value of -0.80%, because the

Downloaded 16 May 2013 to 134.94.122.141. This article is copyrighted as indicated in the abstract. Reuse of AIP content is subject to the terms at: http://jap.aip.org/about/rights_and_permissions

layer is fully strained. At a specific critical thickness, here at about 15 nm for the interface composition, relaxation accompanied by In pulling occurs. The residual strain reaches a maximum value but cannot follow the trend of the nominal strain to higher values. The layer is forced to relax to incorporate more In and hence residual compressive strain cannot exceed the critical value of about 1.1%. This value represents a limitation for compressive strain generation due to In incorporation near the AlInGaN/GaN interface. This relaxation model is confirmed by the results, determined on sample C, which show partial relaxation and was discussed earlier in this work. The nominal strain of sample C of 1.19% exceeds the critical value of 1.1%, and hence, the lattice is forced to relax in order to reduce the strain to a value below 1.1%.

This critical compressive strain value for maximum In incorporation in quaternary AlInGaN, derived from our virtual multi-layer model, might seem quite low, if compared to other devices, i.e., green LED, in which high In contents and strain states are necessary. Here, a detailed discussion of the working principles of GaN-based LED is prevented, but the following should be addressed: Luminescence properties are mainly related to the nanostructure of the material.[23,35–39] The appearance of composition and strain fluctuations on the nanoscale lead to improved carrier confinement in band tail states, which dominate the luminescence spectra. The average composition, which is determined by the measurement techniques discussed in this paper, cannot directly be correlated to these luminescence spectra. Hence, the proposed critical compressive strain value at an interface is determined by taking a homogeneous layer in lateral dimensions into account.

The correlation between relaxation and crystal quality can be investigated further by having a closer look at the RBS channeling spectrum in Figure 6. A more detailed examination of the In signal of the channeling spectrum reveals a significantly different shape than for the random spectrum with a clear peak shape with the peak maximum at the depth, at which the In content is reaching its maximum. This behavior can be described by the multi-layer relaxation model as follows: Starting fully strained on the GaN buffer, the lattice constant is continuously changing after 10 nm to 15 nm due to relaxation. This increases disorder and inhomogeneity in the layer, so that the channeling signal increases. The maximum, which corresponds to the lowest crystal quality in this sample, is observed at that point, at which the In content saturates and the layer is fully relaxed. Subsequently, the In content remains constant, which slightly improves crystal quality and lets us observe a now decreasing channeling signal.

IV. CONCLUSION

We discussed structural properties of tensile and compressively strained quaternary AlInGaN layers on GaN buffer structures. The influence of the reactor pressure and growth surface temperature on composition, strain, and crystal quality was investigated. While the reactor pressure has a negligible influence on In incorporation, Al incorporation is strongly suppressed due to gas phase reactions of TMAl. An inferior crystal quality was observed for layers grown at higher pressure, which is caused by the larger lattice mismatch due to the low Al content.

The growth surface temperature determines strongly the desorption rate of In atoms, so that In incorporation can be controlled by the temperature. AlInGaN layers grown at high temperatures above 750 °C exhibit high crystal quality. A reduction of the temperature leads to higher In contents, which result again in larger lattice mismatch and inferior crystal quality.

A virtual multi-layer model with different strain states in each layer is proposed to describe relaxation and In pulling effect in growth direction in compressively strained AlInGaN. The critical strain value for maximum In incorporation was determined to be at 1.1%, which is a limit for compressive strain generated by pseudomorphic growth near the AlInGaN/GaN interface. Relaxation is accompanied by In pulling and degrades homogeneity in growth direction and hence crystal quality. Tensile strained layers up to values of 0.96% can be grown thicker (up to minimum 70 nm) without relaxation.

The limitation of average strain generation at interfaces in laterally homogeneously nitride layers grown on GaN should be kept in mind while designing strain-induced polarization-engineered devices like GaN-based HEMT or LED.

ACKNOWLEDGMENTS

This work was sponsored by the DFG (Deutsche Forschungsgemeinschaft).

[1] O. Ambacher *et al.*, "Pyroelectric properties of Al(In)GaN/GaN hetero- and quantum well structures," J. Phys.: Condens. Matter **14**, 3399–3434 (2002).
[2] V. Fiorentini *et al.*, "Effects of macroscopic polarization in III-V nitride multiple quantum wells," Phys. Rev. B **60**, 8849 (1999).
[3] M. Gonschorek *et al.*, "High electron mobility lattice-matched AlInN/GaN field-effect transistor heterostructures," Appl. Phys. Lett. **89**, 062106 (2006).
[4] S. Nakamura *et al.*, "High-brightness InGaN blue, green and yellow light-emitting diodes with quantum well structures," Jpn. J. Appl. Phys. **34**, L797–L799 (1995).
[5] Y. Liu *et al.*, "Growth and characterization of high-quality quaternary AlInGaN epilayers on sapphire," J. Cryst. Growth **259**, 245 (2003).
[6] Y. Kobayashi *et al.*, "Structural and optical properties of AlGaInN/GaN grown by MOVPE," Jpn. J. Appl. Phys. **42**, 2300 (2003).
[7] N. Ketteniss *et al.*, "Study on quaternary AlInGaN/GaN HFETs grown on sapphire substrates," Semicond. Sci. Technol. **25**, 075013 (2010).
[8] N. Ketteniss *et al.*, "Polarization-reduced quaternary InAlGaN/GaN HFET and MISHFET devices," Semicond. Sci. Technol. **27**, 055012 (2012).
[9] H. Hahn *et al.*, "First polarisation-engineered compressively strained AlInGaN barrier enhancement-mode MISHFET," Semicond. Sci. Technol. **27**, 055004 (2012).
[10] S. Park *et al.*, "Light emission enhancement in blue InGaAlN/InGaN quantum well structures," Appl. Phys. Lett. **99**, 181101 (2011).
[11] M. Jetter *et al.*, "MOVPE grown quaternary AlInGaN layers for polarization matched quantum wells and efficient active regions," Phys. Status Solidi C **8**(7-8), 2163–2166 (2011).
[12] M. Kamp *et al.*, "Fundamentals, materials properties and device performances in GaN MBE using on-surface cracking of ammonia," J. Nitride Semic. MRS **2**, 26 (1997).
[13] B. Holländer *et al.*, "New high-precision 5-axes RBS/channeling goniometer for ion beam analysis of 150 mm wafers," Nucl. Instrum. Methods Phys. Res. B **161–163**, 227–230 (2000).
[14] J. R. Creighton *et al.*, "Nature of the parasitic chemistry during AlGaInN OMVPE," J. Cryst. Growth **261**, 204–213 (2004).
[15] A. V. Lobanova *et al.*, "Effect of V/III ratio in AlN and AlGaN MOVPE," J. Cryst. Growth **287**, 601–604 (2006).

Downloaded 16 May 2013 to 134.94.122.141. This article is copyrighted as indicated in the abstract. Reuse of AIP content is subject to the terms at: http://jap.aip.org/about/rights_and_permissions

[16]F. Nakamura *et al.*, "AlN and AlGaN growth using low-pressure metalorganic chemical vapor deposition," J. Cryst. Growth **195**, 280–285 (1998).
[17]D. Holec, "Critical thickness calculations for InGaN/GaN," J. Cryst. Growth **303**, 314–317 (2007).
[18]J. E. Northrup *et al.*, "Surface energetics, pit formation, and chemical ordering in InGaN alloys," Appl. Phys. Lett. **74**, 2319 (1999).
[19]B. Reuters *et al.*, "Growth studies on quaternary AlInGaN layers for HEMT application," J. Electron. Mater. **41**(5), 905–909 (2012).
[20]K. Lorenz, "Relaxation of compressively strained AlInN on GaN," J. Cryst. Growth **310**, 4058–4064 (2008).
[21]T. Takayama *et al.*, "Analysis of phase-separation region in wurtzite group III nitride quaternary material system using modified valence force field model," J. Cryst. Growth **222**, 29–37 (2001).
[22]R. A. Oliver *et al.*, "Growth modes in heteroepitaxy of InGaN on GaN," J. Appl. Phys. **97**, 013707 (2005).
[23]S. Pereira *et al.*, "Role of nanoscale strain inhomogeneity on the light emission from InGaN epilayers," Adv. Funct. Mater. **17**, 37–42 (2007).
[24]E. Sakalauskas *et al.*, "Dielectric function and optical properties of quaternary AlInGaN alloys," J. Appl. Phys. **110**, 013102 (2011).
[25]K. Wang, "Optical energies of AlInN epilayers," J. Appl. Phys. **103**, 073510 (2008).
[26]W. Terashima *et al.*, "Growth and characterization of AlInN ternary alloys in whole composition range and fabrication of InN/AlInN multiple quantum wells by RF molecular beam epitaxy," Jpn. J. Appl. Phys. **45**(21), L539–L542 (2006).
[27]E. Iliopoulos *et al.*, "Energy bandgap bowing of InAlN alloys studied by spectroscopic ellipsometry," Appl. Phys. Lett. **92**, 191907 (2008).
[28]A. Polian *et al.*, "Elastic constants of GaN," J. Appl. Phys. **79**, 3343 (1996).
[29]A. F. Wright *et al.*, "Elastic properties of zinc-blende and wurtzite AlN, GaN and InN," J. Appl. Phys. **82**(6), 2833 (1997).
[30]M. Lopuszynski *et al.*, "Composition dependence of elastic constants in wurtzite AlGaInN alloys," J. Appl. Phys. **111**, 033502 (2012).
[31]S. Pereira *et al.*, "Compositional pulling effects in InGaNGaN layers: A combined depth-resolved cathodoluminescence and Rutherford backscattering/channeling study," Phys. Rev. B **64**, 205311 (2001).
[32]P. Boguslawski *et al.*, "Surface segregation and interface stability of AlN/GaN, GaN/InN, and AlN/InN {0001} epitaxial systems," Phys. Rev. B **61**, 10820 (2000).
[33]U. Großner *et al.*, "Initial stages of III-nitride growth," Appl. Phys. Lett. **74**, 3851 (1999).
[34]S. Pereira *et al.*, "Interpretation of double X-ray diffraction peaks from InGaN layers," Appl. Phys. Lett. **79**, 1432 (2001).
[35]K. P. O'Donnell *et al.*, "Origin of luminescence from InGaN diodes," Phys. Rev. Lett. **82**, 237–240 (1999).
[36]C.A. Tran *et al.*, "Phase separation in InGaN/GaN multiple quantum wells and its relation to brightness of blue and green LEDs," J. Cryst. Growth **195**, 397–400 (1998).
[37]T. Mukai *et al.*, "Current and temperature dependence of electroluminescence of InGaN-based UV/blue/green light-emitting-diodes," Jpn. J. Appl. Phys. **37**, 1358–1361 (1998).
[38]C. A. Parker *et al.*, "Determination of the critical layer thickness in the InGaN/GaN heterostructures," Appl. Phys. Lett. **75**, 2776–2778 (1999).
[39]J. R. Jinschek *et al.*, "Local In segregation and bandgap variations in high efficiency green light emitting InGaN/GaN diodes," Solid State Commun. **137**, 230–234 (2006).

Downloaded 16 May 2013 to 134.94.122.141. This article is copyrighted as indicated in the abstract. Reuse of AIP content is subject to the terms at: http://jap.aip.org/about/rights_and_permissions